J Musculoskelet Neuronal Interact 2013; 13(2):178-184

Original Article

Hylonome

Time-dependent effects of sclerostin antibody on a mouse fracture healing model

L. Cui[1]*, H. Cheng[2]*, C. Song[3], C. Li[4], W.S. Simonet[4], H.Z. Ke[4], G. Li[3,5]

[1]Guangdong Key Laboratory for R&D of Natural Drug, Guangdong Medical College, Zhanjiang 524023, Guangdong, PR China; [2]Department of Pathology, State Key Laboratory of Cancer Biology, Xijing Hospital and School of Basic Medicine, Fourth Military Medical University, Xi'an, Shaanxi 710032, P.R. China; [3]Stem Cell and Regeneration Program, Li Ka Shing Institute of Health Sciences, School of Biomedical Sciences and The Department of Orthopaedics and Traumatology, The Chinese University of Hong Kong, Shatin, N.T., Hong Kong, SAR China; [4]Metabolic Disorders, Amgen Inc., One Amgen Center Dr., Thousand Oaks, California, 91320 USA; [5]The Chinese University of Hong Kong Shenzhen Research Institute, Nanshan District, Shenzhen, PR China

* These authors contributed equally and served as co-first author

Abstract

Objectives: Treatment with Sclerostin antibody (Scl-Ab) has shown to enhance fracture healing in rodent and non-human primate models. The current study investigated the time-dependent changes during Scl-Ab treatment in a mouse osteotomy model. **Methods:** 1 day after osteotomy, C57BL mice received subcutaneous injection with vehicle or Scl-Ab at 25 mg/kg, twice/week for 2, 4, or 6 weeks. 20 mice from each group were necropsied at weeks 2, 4, and 6 for Micro-CT, histomorphmetry and mechanical testing examinations. **Results:** The bone mineral apposition rate at fracture callus was significantly higher in the Scl-Ab treated groups at all the time points. Micro-CT analysis showed that the volumetric bone mineral density (vBMD) and bone volume over tissue volume (BV/TV) in the Scl-Ab treated groups at 4 and 6 weeks were significantly greater than that of vehicle control groups. Mechanical testing showed that the maximum load of failure at the fracture callus increased significantly by 68% at 6 weeks in the Scl-Ab treated groups. **Conclusions:** This study confirmed that mice treated with Scl-Ab increased bone formation from 2 weeks, bone mineral density and bone volume at 4 weeks, followed by significant increase in bone strength at the fracture site at 6 weeks. These results suggest that applying sclerostin antibody at early stage fracture healing promotes fracture healing.

Keywords: Sclerostin Antibody, Fracture Healing, Bone Formation, Mice

Introduction

Fracture healing is a biological process consisting inflammation, repair and bone remodeling phases. 5-10% of fractures may result in impaired healing due to high-energy trauma, infection, soft-tissue defect, causing pain and suffer to patients and greater health care burdens to the society[1]. Surgical managements including bone grafting, growth factor treatments (bone morphogenetic proteins) and stem cell therapy have all been tried, but with limited success[1]. Most of the current therapies for promoting fracture healing require either invasive procedures (bone grafting, biomaterial implantation) associated with risks of complications[2]. There is a need for non-invasive, systemic therapy to enhance fracture healing.

Sclerostin, a protein secreted primarily by osteocytes, is a negative regulator of bone formation[3-6]. Sclerostin is the product of the SOST gene and mutations of the SOST gene causes

CYL, WSS and HZK are employees of Amgen and own Amgen stocks. GL received research funding from Amgen Inc., USA. Research was funded by Amgen Inc., USA. These works were also supported in part by the National Basic Science and Development Programme (973 Programme, 2012CB518105).

Corresponding authors:
Prof. Gang Li, MBBS, PhD, Room 904, Li Ka Shing Institute of Health Sciences, The Chinese University of Hong Kong, Prince of Wales Hospital, Shatin, N.T., Hong Kong, SAR China
E-mail: gangli@cuhk.edu.hk
Dr. H. Z. Ke, Metabolic Disorders, Amgen Inc., One Amgen Center Dr., Thousand Oaks, California, 91320 U.S.A.
E-mail: hke@amgen.com

Edited by: F. Rauch
Accepted 27 March 2013

increased bone formation and high bone mass in humans[3,4]. Similarly, a high bone mass phenotype is replicated in SOST knockout mice[7]. Sclerostin is reported to bind the LRP5/6 receptor, thus antagonizing Wnt signaling and increasing β-catenin degradation[8]. It was recently reported that sclerostin monoclonal antibody (Scl-Ab) treatment increase bone formation, bone mass, and bone strength in animal model of postmenopausal osteoporosis[9-10]; and increased bone formation markers and BMD in humans[11]. In addition, it has been shown that Scl-Ab enhances bone healing and improves bone density and strength of non-fractured bones in animal models[12]. However, studies reported in animal models of fracture healing with Scl-Ab had only showed the later healing response. No time-dependent study has been reported for the effects of Scl-Ab on bone healing. The aim of this study was to determine the time-dependent changes induced by Scl-Ab during fracture repair in a mouse femoral osteotomy model. Time points of 2, 4 and 6 weeks were employed to determine the early and late response to Scl-Ab treatment in this model.

Materials and methods

Animal model of femoral osteotomy

120 male C57BL mice (8-10 weeks old; body weight: 35 to 40g) were used for this study. All animals were housed in a designated and Hong Kong government approved animal facility at The Chinese University Hong Kong, in according to The Chinese University Hong Kong's animal experimental regulations.

A model of mouse femoral osteotomy was briefly presented as follows. General anesthesia was induced using a gaseous mixture of 3% isofluorane in a 50:50 mixture of N2O2:O2 at 2L/minute in a sealed chamber. Once asleep animals were transferred to the operating table with gases delivered using a Hunt mask. A 0.8 mm (diameter) pin (21G needle) was then inserted into the right femoral bone marrow cavity at the distal condyles and then withdrawn (half of the needle length). A lateral approach was used to expose the middle femoral shaft. A transverse osteotomy was then made using a low-speed hand-held saw. Once the bone was cut, the needle was pushed back as far as its tip protruded from the region below the greater trochanter. The needle tip was then bent and buried into the surrounding soft tissue of the greater trochanter; the rest of the needle was then pulled back as tight as possible to reduce the fracture gap; the needle was finally cut at the knee level using a wire cutter. The muscle and skin at the knee level were then sutured.

After osteotomy, the mice were divided into 6 groups: 3 treatment groups (Scl-Ab) and 3 vehicle control (saline) groups, 20 mice per group. The mice were subcutaneously injected with saline vehicle or a murine Scl-Ab at 25 mg/kg, twice per week, starting one day post-osteotomy. Groups of Scl-Ab treated and vehicle control mice were terminated at weeks 2, 4 and 6. Eight mice from each group were given subcutaneous injections of 10 mg/kg calcein (Sigma Chemical Co., St. Louis, MO, USA), a fluorochrome bone marker, at 12 and 2 days before sacrifice in order to determine dynamic changes in mineral apposition rate in bone tissues. Twelve fractured femurs per group were isolated for 3-point bending mechanical testing and 8 fractured femurs (with the fluorochrome pre-labeled) per group were used for micro-CT examination followed by histology examination.

Radiography analysis

Radiograph was taken at the day of surgery and weekly thereafter until sacrifice. All animals were anaesthetized using gaseous mixture of 3% isofluorane in a 50:50 mixture of N2O2:O2 at 2 L/minutes in a sealed chamber and placed inside a high-resolution digital radiography system (Faxitron MX-20 with DC-2 option, Faxitron x-ray Corporation, Illinois, USA) for radiographic analysis, with an exposure condition of 24 kV for 3 seconds.

Micro-CT examinations

On the day of termination, 8 animals from each group (with the calcein injection) were selected for micro-CT examination. Femurs were collected and soft tissues were removed with care. The specimens were fixed at 10% buffered formalin for 48 hours and then transferred into 70% ethanol before micro-CT examinations. For micro-CT examination, the samples were scanned by a micro-CT machine (μCT40, Scanco Medical, Brüttisellen, Switzerland). The resolution was set at 36 μm per voxel. The three-dimensional (3D) reconstruction of the femur was performed using the software provided. A total of 420 slices (210 slices of each side of the fracture line) were taken. For data analysis, the following parameters were used to generate reports (from longitudinal sections): mean volumetric bone mineral density (BMD), bone mineral content (BMC), tissue mineral content (TMC), bone volume (BV), tissue volume (TV), trabecular thickness (Calib.Tb.Th.3D) and trabecular space (Calib.Tb.Sp.3D).

Histomorphometry analysis

After non-destructive examinations, the fractured femurs (8 from each group) were then embedded with methyl methacrylate as described below. Samples were then sectioned at 300 μm thickness by a saw microtome (SP1600, Leica Microsystems GmbH, Wetzlar, Germany) sagittally and three sections from middle one-third of each sample were further ground and polished to 100±10 μm thickness using a grinder/polishing machine (Phoenix 4000, Buehler Ltd, Lake Bluff, IL, USA). The newly formed bone was determined by the distance between the two fluorochrome labels using epifluorescent microscopy (DMRXA2 imaging system, Leica Microsystems GmbH, Wetzlar, Germany). Measurements of distance were performed in the well-organized trabecular bone areas of the fracture callus. 5 regions were randomly measured for each sample, and epifluorescent micrographs were taken under a red and green filter separately (16 x magnification) and merged by PhotoStitch 3.1 (Canon Inc, Tokyo, Japan). Image was performed by two investigators in a blinded manner. The bone mineralization/apposition rate was calculated by the distance (between the two labels) divided by 10 days (the time between the two labels), and expressed as mm/day.

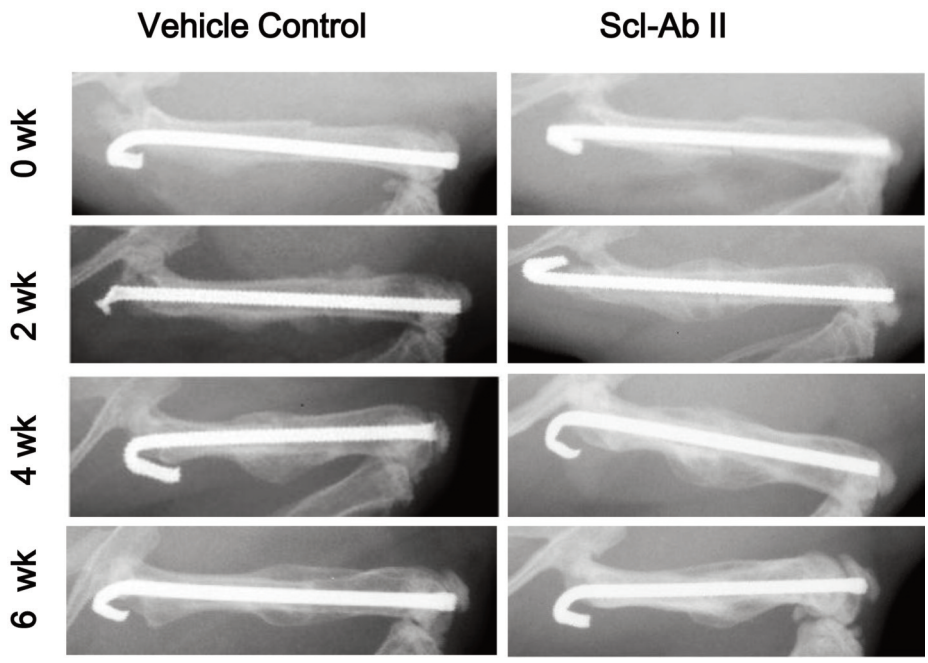

Figure 1. Representative radiographs of fractured femurs from mice treated with Scl-Ab or vehicle at 2, 4 and 6 weeks. Radiograph was carried out weekly after osteotomy. At 2 weeks, the group received Scl-Ab had larger callus area than that of the vehicle control group. At 4 and 6 weeks, the size of callus in the control group continued to increase, while the Scl-Ab treatment groups had showed advanced callus remodeling, indicating a faster fracture union in the Scl-Ab treatment groups.

Mechanical testing

At 2, 4, and 6 weeks after osteotomy, 12 mice from each groups were sacrificed and both fractured and non-fractured contralateral femurs were isolated. The internal fixation needle and soft tissues were carefully removed with minimal disruption of the structural integrity of the fracture. The femurs were then placed on two lower supports that were 8 mm apart and the loading force was applied at 5 mm/minute at the mid-diaphysis on the anterior surface of the femur such that the posterior surface was in tension. Maximal load of failure and the ratio (fractured femur/contralateral intact femur) of maximal load of failure was then calculated to normalize the variations among the samples/animals.

Histology examination

After the micro-CT examination, the specimens were processed and embedded in methyl-methacrylate (MMA). The infiltration process was carried out by placing the bone specimens into a solution of MMA and dibutylphtalate (3:1) for 48 hours, followed by another 48 hours in MMA. Embedding of the infiltrated specimens was done in fresh MMA, dibutylphtalate (3:1) and 2.5% benzoyl peroxide solution at room temperature. Polymerization was completed within 48 hours. Attempts were made to standardize the sectioning at a mid-sagittal plane of each specimen by cutting the specimen in half (longitudinally in a sagittal plane) using a low-speed diamond saw, and the MMA sections were then polished to thin MMA sections (20 μm). For histology examination, MMA resin was removed by immersing the slides in methoxyethyl acetate at room temperature. Slices were then taken through graded ethanols and distilled water, then stained with Stevenel's Blue, and counter stained with Van Gieson stain.

Statistical analysis

Quantitative data were analyzed using a commercially available statistical program SPSS (Version 16, Chicago, Illinois, USA). Student's t-Test was employed to compare the difference between vehicle and Scl-Ab treated groups at each time point, and $p<0.05$ was considered statistically significant.

Results

X-ray analysis

Digital x-rays of representative animals from each group are shown in Figure 1. At 2 weeks, the callus size in mice received Scl-Ab appeared larger than that of the vehicle control group. At 4 and 6 weeks, the size of callus in the control group continued to increase, while it was gradually reduced in the Scl-Ab groups, indicating a rapid callus remodeling and a faster fracture union in the Scl-Ab treated groups at weeks 4 and 6.

Micro-CT examinations

Mean volumetric bone mineral density (vBMD) in the 4 and 6 week Scl-Ab-treated groups was significantly higher than

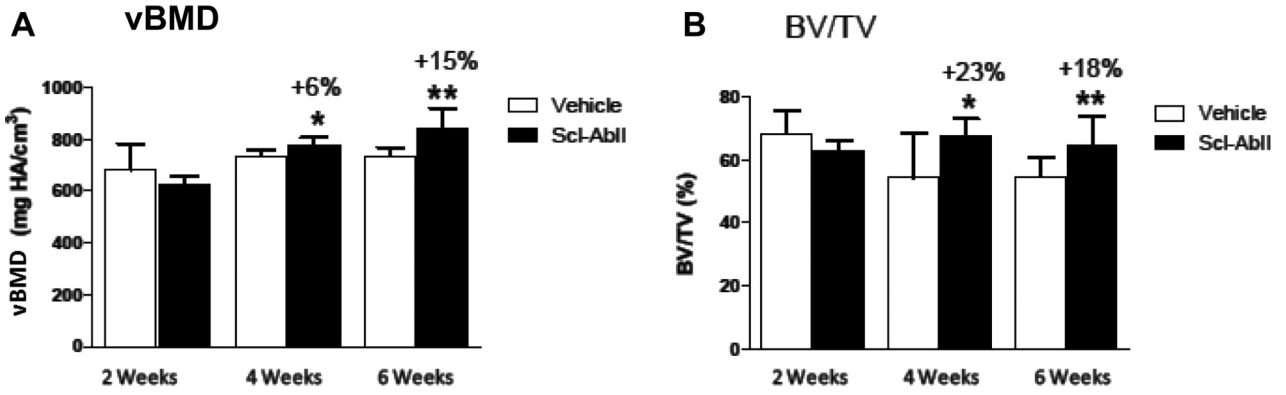

Figure 2. A. Micro-CT analysis was performed, volumetric bone mineral density (v-BMD) in the Scl-AbII treated groups at 4 and 6 weeks were significantly higher than the vehicle groups respectively (*p<0.005; **p<0.001). **B.** The percentage of bone volume (BV) in tissue volume (TV), which was represented as BV/TV in the Scl-Ab treated groups were also significantly higher than that of the control groups at 4 and 6 weeks respectively. T-tests were used to determine significant difference between the vehicle and Scl-Ab groups at each time point.

their respective vehicle control groups (*p<0.003; and **p<0.007 respectively, Student's t-test), while there was no significant difference between the treated and controls at week 2 (Figure 2A). The percentage of bone volume over tissue volume (BV/TV) showed the similar pattern. BV/TV in the 4 and 6 week Scl-Ab treated groups was significant greater than their respective vehicle control groups (*p<0.02 and **p<0.03 respectively, Figure 2B).

Mechanical testing

As shown in Figure 3, maximal loading was significantly increased (+68%) in the 6 week Scl-Ab-treated group versus the vehicle control group (*p<0.02). Maximal loading was non-significantly increased (28%) in the 4 week Scl-Ab treated group versus the vehicle control group. When comparing the ratios of fractured femurs with the intact ones, maximal loading ratio in the group treated with Scl-Ab for 6 weeks was significantly greater than the vehicle-treated control group at 6 weeks (*p<0.01).

Histomorphometry and histology examinations

At 2 weeks, the total callus areas in the Scl-Ab treated group were greater than that in vehicle controls as shown by 3D construction images of micro CT examination (Figures 4 A, D) and HE sections (Figures 4 A', D'). At 4 weeks of treatment, more bony tissue was seen in the Scl-Ab treated group than that of the vehicle group (Figures 4 B, B', E, E'). The callus became more mature at 6 weeks in the Scl-Ab treated group comparing to the vehicle group (Figures 4 C', F'). More new bone formation was observed in the Scl-Ab treated groups at all-time points than their respective vehicle control groups on the MMA sections with the newly formed bone being labeled by fluorochromes. The bone mineral apposition rate as demonstrated by the measurement of the two calcein labels, was significantly greater in the Scl-Ab treated groups at all time points compared to their respective vehicle control groups (Figure 5).

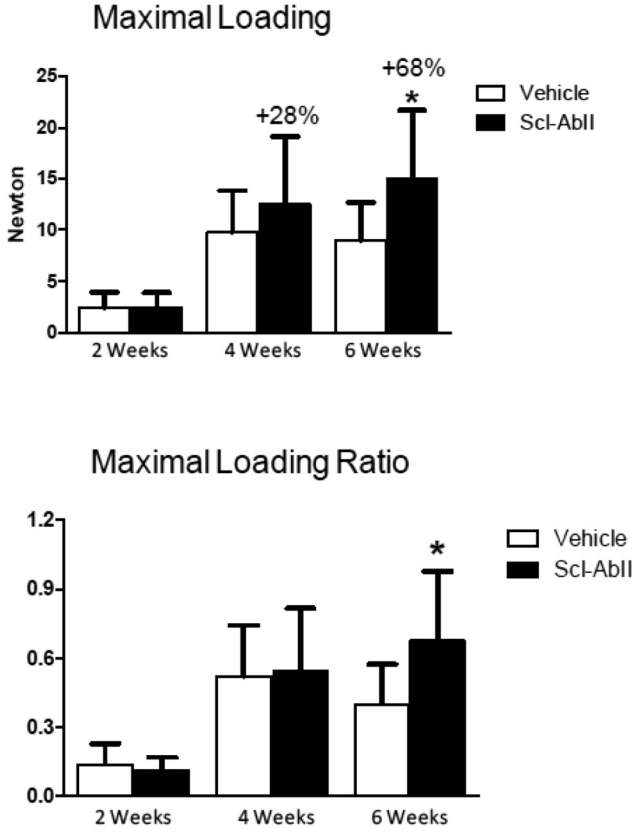

Figure 3. Mechanical testing results showed that at 2 and 4 weeks after fracture, there was no significant difference in maximal loading between the Scl-Ab treatment groups and vehicle control groups. At 6 weeks, the maximal loading in the Scl-Ab treatment group was significantly (1.68-fold) stronger than the vehicle-treated group (*p<0.05). Maximal loading ratio in the group treated with Scl-Ab for 6 weeks was also significantly greater than the vehicle-treated control group (*p<0.01). T-tests were used to determine significant difference between the vehicle and Scl-Ab groups at each time point.

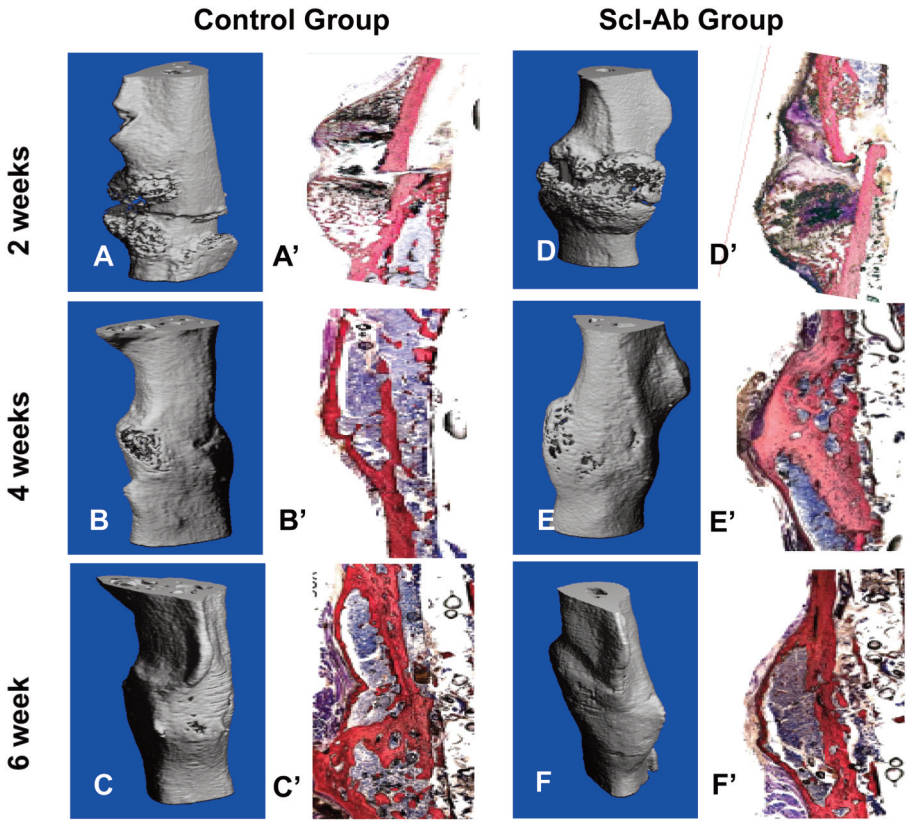

Figure 4. Representative 3D microCT reconstruction images (**A-F**) and MMA sections showed the histology of the fractured femurs (A'-F') of Scl-Ab and vehicle treated groups at 2, 4 and 6 weeks. After 2 weeks of fracture, both vehicle control (A) and Scl-Ab treated (D) groups showed signs of callus formation, the total callus area were greater in the Scl-Ab treatment group (D') comparing to vehicle group (A'). After 4 weeks of treatment, more callus (bone formation) was seen in the Scl-Ab (E') group versus the vehicle control group (B'). At 6 weeks, the remodeling of the fracture callus was more advanced in the Scl-Ab group (F') than that of the vehicle control group (C'). **A'-F'**: Van Gieson staining, the red color staining indicates the mineralized bone, x 16 magnifications.

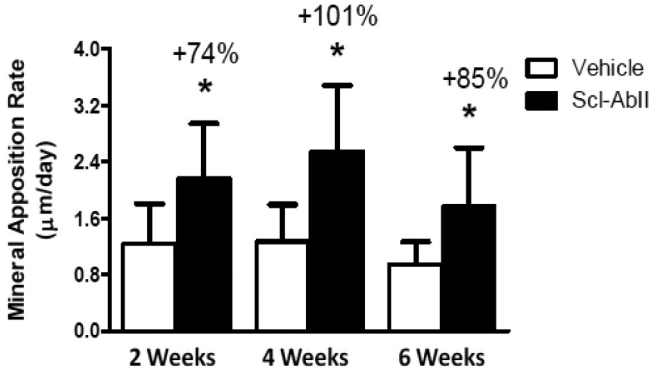

Figure 5. The amount of newly formed bone as highlighted by the fluorescent calcein labelings was greater in the Scl-Ab treated groups than those of vehicle control groups at 2, 4 and 6 weeks after fracture. The mineral apposition rate at the fractured callus was significantly (*p<0.001) higher in the Scl-Ab treated groups comparing to their respective vehicle control groups at each time point. T-tests were used to determine significant difference between the vehicle and Scl-Ab groups at each time point.

Discussion

All animals tolerated well with the antibody treatment and showed no sign of any adverse effect in both controls and Scl-Ab treated groups at all time points. After 4 weeks of antibody treatment, bone formation was enhanced, confirmed by micro-CT quantitative examination, and the maximal loading to failure of the fractured bone was significantly greater after 6 weeks of Scl-Ab treatment. The mineral apposition rate was significantly greater in the Scl-Ab treatment groups at all time points, suggesting Scl-Ab enhanced bone formation through speeding up the bone formation. These findings are in agreement with previous reports that Scl-Ab enhances bone healing[10].

Sclerostin is highly expressed in osteocytes, these cells are the responsive cells for mechanical loading. Sclerostin expression is significantly decreased in the presence of mechanical loading and leading to enhanced osteogenesis[11]. A recent study by Sarahrudi et al.[12] found that strongly enhanced levels of sclerostin during human fracture healing, they found that fracture haematoma contained higher sclerostin concentrations

compared to patient's serum. During the early haematoma (inflammation) phase of fracture, sclerostin first released at the fracture site through the initial trauma and then reaches to the peripheral serum thereafter, and subsequently it may be released from the chondrocytes being broken down during endochondral ossification. Sclerostin may be a by-product (passively released) during the early fracture healing process, it may partially slow down fracture healing, therefore, inhibiting its biological activities by Scl-Ab from the early phase of fracture benefited fracture healing. Increased sclerostin serum levels were also been found to associate with bone formation and resorption markers in patients with immobilization-induced bone loss[13], suggesting that sclerostin plays important roles in regulating bone formation, remodeling and mechanical adaption. The expression of sclerostin in the synovial tissue of patients with rheumatoid arthritis was extremely high, suggesting its release from the surrounding bone and cartilage tissues during inflammatory processes[14], inhibits bone formation; the use of sclerostin antibody to promote bone formation in inflammatory conditions needs further investigation.

In sclerostin knocking out mice, Li et al found that more fracture callus was seen at early stages of fracture healing and greater callus mineral density and strength at later stages of fracture healing[15]. The use of sclerostin antibody resulted in increased bone mass, strength and formation in rat models of ovariostemy and aged male rats[9,16]. Sclerostin antibody could also increase trabecular bone volume and thickness, bone formation rates, and mineralizing bone surfaces in a rat model of hind limb immobilization and compared to normal controls[17]. All these data suggest that systemic use of Scl-Ab during fracture healing is beneficial to reduce the inhibitory effects of sclerostin released during fracture healing courses which are associated with initial trauma to bone; endochondral ossification and bone remodeling, as well as prolonged immobilization of the fractured limb(s).

In conclusion, the present study demonstrated that during 6-week time course, mice treated with Scl-Ab showed a significant improvement in fracture healing, proving the positive role of sclerostin antibody in enhancing/promoting bone repair. Sclerostin antibody may be a potential therapeutic utility in managing bone fracture repair through its early systemic administration.

Reference

1. Zuscik M, O'Keefe RJ. Skeletal healing. In: Rosen CJ, editor. Primer on the Metabolic Bone Diseases and Disorders of Mineral Metabolism. Washington, DC: American Society for Bone and Mineral Research, 2008: p.61-65.
2. Poynton AR, Lane JM. Safety profile for the clinical use of bone morphogenetic proteins in the spine. Spine (Phila Pa 1976) 2002;27:S40-48.
3. Balemans W, Ebeling M, Patel N, Van Hul E, Olson P, Dioszegi M, Lacza C, Wuyts W, Van Den Ende J, Willems P, Paes-Alves AF, Hill S, Bueno M, Ramos FJ, Tacconi P, Dikkers FG, Stratakis C, Lindpaintner K, Vickery B, Foernzler D, Van Hul W. Increased bone density in sclerosteosis is due to the deficiency of a novel secreted protein (SOST). Hum Mol Genet 2001;10:537-43.
4. Brunkow ME, Gardner JC, Van Ness J, Paeper BW, Kovacevich BR, Proll S, Skonier JE, Zhao L, Sabo PJ, Fu Y, Alisch RS, Gillett L, Colbert T, Tacconi P, Galas D, Hamersma H, Beighton P, Mulligan J. Bone dysplasia sclerosteosis results from loss of the SOST gene product, a novel cysteine knot-containing protein. Am J Hum Genet 2001;68:577-89.
5. Poole KE, van Bezooijen RL, Loveridge N, Hamersma H, Papapoulos SE, Löwik CW, Reeve J. Sclerostin is a delayed secreted product of osteocytes that inhibits bone formation. FASEB J 2005;19:1842-4.
6. Winkler DG, Sutherland MK, Geoghegan JC, Yu C, Hayes T, Skonier JE, Shpektor D, Jonas M, Kovacevich BR, Staehling-Hampton K, Appleby M, Brunkow ME, Latham JA. Osteocyte control of bone formation via sclerostin, a novel BMP antagonist. EMBO J 2003;22:6267-6.
7. Li X, Ominsky MS, Niu QT, Sun N, Daugherty B, D'Agostin D, Kurahara C, Gao Y, Cao J, Gong J, Asuncion F, Barrero M, Warmington K, Dwyer D, Stolina M, Morony S, Sarosi I, Kostenuik PJ, Lacey DL, Simonet WS, Ke HZ, Paszty C. Targeted Deletion of the Sclerostin Gene in Mice Results in Increased Bone Formation and Bone Strength. J Bone Miner Res 2008;23:860-9.
8. ten Dijke P, Krause C, de Gorter DJJ, Lowik Clemens WGM, van Bezooijen RL. Osteocyte-derived sclerostin inhibits bone formation: its role in bone morphogenetic protein and Wnt signaling. J Bone Joint Surg Am 2008; 90(Suppl.1):31-5.
9. Li X, Ominsky MS, Warmington KS, Morony S, Gong J, Cao J, Gao Y, Shalhoub V, Tipton B, Haldankar R, Chen Q, Winters A, Boone T, Geng Z, Niu QT, Ke HZ, Kostenuik PJ, Simonet WS, Lacey DL, Paszty C. Sclerostin antibody treatment Increases bone formation, bone mass and bone strength in a rat model of postmenopausal osteoporosis. J Bone Miner Res 2009;24:578-88.
10. Ominsky MS, Li CY, Li XD, Tan HL, Lee E, Barrero M, Asuncion FJ, Dwyer D, Han CY, Vlasseros F, Samadfam R, Jolette J, Smith SY, Stolina M, Lacey DL, Simonet WS, Paszty C, Li G, Ke HZ. Inhibition of Sclerostin by monoclonal antibody enhances bone healing and improves bone density and strength of non-fractured bones. J Bone Miner Res 2011;26:1012-21.
11. Rbling AG, Bellido T, Turner CH. Mechanical stimulation *in vivo* reduces osteocyte expression of sclerostin. J Musculoskelet Neuronal Interact 2006;6:354.
12. Sarahrudi K, Thomas A, Albrecht C, Aharinejad S. Strongly enhanced levels of sclerostin during human fracture healing. J Orthop Res 2012; DOI 10.1002/jor.22129.
13. Gaudio A, Pennisi P, Bratengeier C, Torrisi V, Lindner B, Mangiafico RA, Pulvirenti I, Hawa G, Tringali G, Fiore CE. Increased sclerostin serum levels associated with bone formation and resorption markers in patients with

immobilization-induced bone loss. J Clin Endocrinol Metab 2010;95:2248-3353.
14. Wehmeyer C, Stratis A, Pap T, Dankbar B. The Role of the WNT inhibitor sclerostin in rheumatoid arthritis. Ann Rheum Dis 2010; 69(Suppl.2):A1-A76.
15. Li C, Ominsky MS, Tan HL, Barrero M, Niu QT, Asuncion FJ, Lee E, Liu M, Simonet WS, Paszty C, Ke HZ. Increased callus mass and enhanced strength during fracture healing in mice lacking the sclerostin gene. Bone 2011;49:1178-85.
16. Li X, Warmington KS, Niu QT, Asuncion FJ, Barrero M, Grisanti M, Dwyer D, Stouch B, Thway TM, Stolina M, Ominsky MS, Kostenuik PJ, Simonet WS, Paszty C, Ke HZ. Inhibition of sclerostin by monoclonal antibody increases bone formation, bone mass, and bone strength in aged male rats. J Bone Miner Res 2010;25:2371-80.
17. Tian X, Jee WS, Li X, Paszty C, Ke HZ. Sclerostin antibody increases bone mass by stimulating bone formation and inhibiting bone resorptin in a hindlimb-immobilization rat model. Bone 2011;48:197-201.